



Echoes of change: lung ultrasound revolutionizing neonatal and pediatric respiratory care

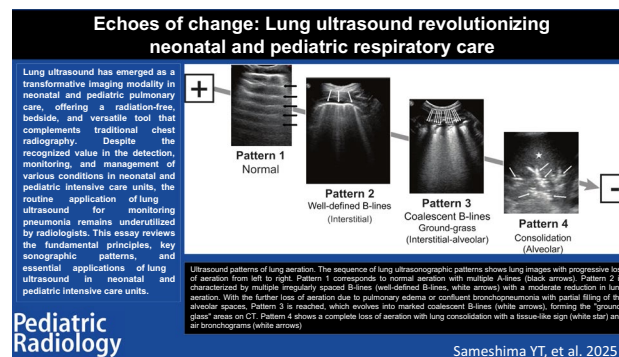
Yoshino Tamaki Sameshima¹ · Andrés García-Bayce² · Fabiana Gual Oranges¹ · Marcelo Assis Rocha¹ · Márcia Wang Matsuoka¹ · Jovan Lovrenski^{3,4}

Received: 26 October 2024 / Revised: 30 May 2025 / Accepted: 2 June 2025
© The Author(s), under exclusive licence to Springer-Verlag GmbH Germany, part of Springer Nature 2025

Abstract

Lung ultrasound has emerged as a transformative imaging modality in neonatal and pediatric pulmonary care, offering a radiation-free, bedside, and versatile tool that complements traditional chest radiography. Despite its recognized value in the detection, monitoring, and management of various conditions in neonatal and pediatric intensive care units, the routine application of lung ultrasound for monitoring pneumonia remains underutilized by radiologists. In recent years, lung ultrasound has demonstrated its effectiveness in monitoring disease progression without the need for repeated chest computed tomography scans, particularly in cases of complicated pneumonia. This essay reviews the fundamental principles, key sonographic patterns, and essential applications of lung ultrasound in neonatal and pediatric intensive care units. Case-based experiences are shared to illustrate how lung ultrasound is shaping clinical decision-making and redefining best practices in pulmonary care by minimizing invasive procedures and reducing radiation exposure.

Graphical Abstract



Keywords Children · Intensive care units, neonatal · Intensive care units, pediatric · Lung · Pneumonia · Pneumothorax · Respiratory distress syndrome · Ultrasonography

Introduction

Chest radiography remains the traditional first-choice method for diagnosing lung diseases in children. It is well known that air interrupts the path of the ultrasound beam and generates multiple reverberation artifacts. This limitation has delayed and restricted the adoption of lung ultrasonography for many years compared to other routinely

used sonographic examinations. While lung ultrasound has long been used in intensive care units [1, 2], its prominence has increased during the COVID-19 pandemic, demonstrating effectiveness in assessing and monitoring the aeration patterns of the lung parenchyma in both children and adults affected by the virus [3–5].

The classic indication for chest ultrasound is the evaluation of pleural effusions, allowing for sonographic-guided thoracentesis when necessary. Nowadays, there is a wide

Extended author information available on the last page of the article

range of possible applications for diseases affecting the peripheral lung parenchyma, pleura, and chest wall, addressing the need to reduce ionizing radiation exposure in neonates and children (following the as low as reasonably achievable (ALARA) and Image Gently principles) [6]. Ultrasound is a safe imaging solution as it is free of ionizing radiation and can be performed at the bedside, thus eliminating the need for patient transportation or stabilization, an important advantage over computed tomography (CT). Furthermore, ultrasound is a cost-effective and readily available imaging modality that provides real-time results. Lung ultrasound is shaping clinical decision-making and redefining best practices in pediatric pulmonary care by minimizing invasive procedures and radiation exposure, reserving chest CT for cases with inadequate or unfavorable clinical progression.

Choosing the right transducer

The selection of the appropriate transducer depends on the age and size of the child. Three types of transducers are most commonly used for chest ultrasound in children:

- (a) *Microconvex of 8–5 MHz* that facilitates lung access for intercostal spaces, subdiaphragmatic access, and through the suprasternal notch. In case a microconvex probe cannot be provided, a regular convex probe (5–2 MHz) will also enable a quality transabdominal (subdiaphragmatic) approach to the lung bases.
- (b) *Linear transducer of 12–7 MHz* is used to assess the chest wall and the lung pleural interface. Irregularities and small subpleural consolidations are better characterized by using this transducer for a detailed evaluation of lung parenchyma. Small areas of necrosis or liquefaction also become more clearly defined with its use.
- (c) *Convex transducer of 5–2 MHz* is a lower-frequency transducer used in older children to provide a broader view of pleural effusion and the extent of lung involvement in extensive pneumonia.

In many cases, the sick child already has a chest radiography, which can guide the sonographic study to the affected area. Occasionally, however, it is necessary to examine the entire chest to identify a focus of consolidation in a suspected infectious process that may not be visible on the chest radiograph. The study usually consists of probing each intercostal space: anterior, lateral, and posterior, along the mid-clavicular line, anterior and posterior axillary lines, bilaterally, as well as in the parasternal and paravertebral regions, if

the patient's clinical condition permits (see [7–10] for more details on thoracic access description).

Fundamental concepts for the understanding of lung ultrasound

A comprehensive understanding of specific concepts and findings is essential for the performance of lung ultrasound. Furthermore, adhering to established protocols and guidelines [11] is crucial for success, including the selection of the probe, the child's positioning, the examination technique, and other nuances inherent to lung ultrasound examinations, particularly in the context of neonatal and pediatric intensive care units. Important practices include probe disinfection to prevent cross-contamination and the sterile warming of gel. It is also essential to select the appropriate preset, depth, and focus settings in case the lung ultrasound preset is unavailable. Employing both transabdominal (subcostal) and standard transthoracic approaches in conjunction can enhance the sensitivity of lung ultrasound in recognizing pathological findings [12].

Notably, lung ultrasound is one of the few ultrasound applications that do not require the latest ultrasound devices, as it relies on detecting artifacts that necessitate deactivating compound filters and harmonics [13, 14]. For additional aspects of the protocol, see the *Lung Ultrasound Consensus Protocol and Guidelines* [11].

Essential lines, signs, and clues for lung ultrasound interpretation

- (a) The *pleural line* is a markedly hyperechogenic continuous horizontal line immediately beneath the ribs that slides while breathing. It represents the pleura-lung interface (Fig. 1).
- (b) *A-lines* consist of multiple hyperechogenic horizontal artifacts seen as a series of equidistant echogenic parallel lines below the pleural line. These represent reverberation artifacts caused by a normal acoustic pleura-lung interface (Fig. 2).
- (c) *B-lines* are vertically oriented artifacts that originate at the pleural line and extend to the bottom of the screen without fading, moving in synchrony with the lung's sliding. Multiple B-lines indicate interstitial/alveolar-interstitial processes; however, the B-line pattern alone does not differentiate the etiology of the interstitial abnormality (Figs. 3 and 4) [15]. The etiology may be pulmonary edema, interstitial pneumonia, or pulmonary fibrosis, among others.
- (d) *Lung sliding* is observed from the back-and-forth movement of the hyperechogenic pleural line during the respiratory motion [1] (Supplementary Material 1). The

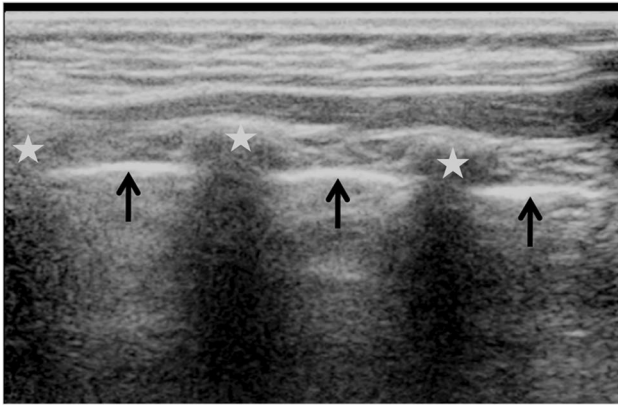


Fig. 1 Longitudinal ultrasound of the anterior left mid-chest in a 2-year-old female, performed using a linear high-frequency transducer (12–5 MHz), demonstrates the *pleural line* as a continuous hyperechoic line representing the pleura-lung interface (*arrows*) immediately beneath the ribs (*stars*), which slides during respiratory motion

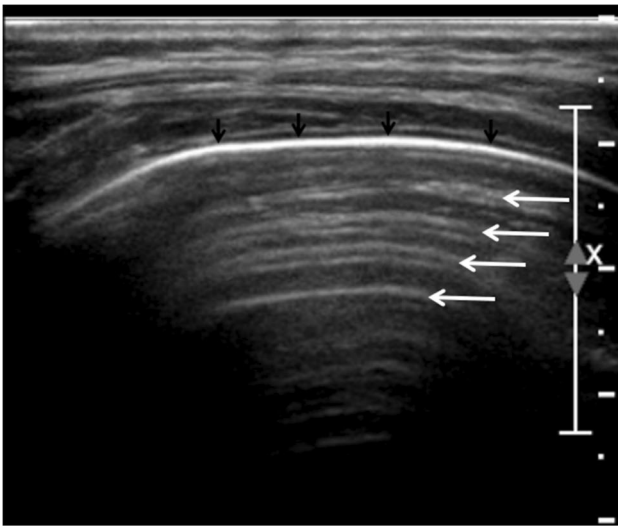


Fig. 2 *A-lines* manifest as multiple artifactual hyperechoic equidistant lines (*white arrows*) parallel to the pleural line (*black arrows*) and are present in normal aerated lungs. This transverse ultrasound image was obtained from the anterior region of the right mid-chest in a 15-month-old male using a high-frequency linear transducer (12–5 MHz)

amplitude of the lung sliding is minimal at the apices and maximal at the bases. M-mode ultrasound can also document this sign, revealing the seashore sign. In M-mode, the motionless chest wall is represented by horizontal lines, while the deeper part below the pleural line produces a sandy pattern with motion artifacts, the *seashore sign* (Fig. 5).

- (e) *Lung pulse* is the vertical movement of the pleural line synchronous with cardiac movements transmitted by a

consolidated lung or atelectasis [16] (Supplementary Material 2).

- (f) *Tissue-like sign* refers to the characteristic appearance of pulmonary consolidation, where the echogenicity of the lung parenchyma resembles that of the liver or spleen parenchyma [17–19] (Fig. 6).
- (g) *Fluid color sign* is the color Doppler signal in the pleural effusion that results from transmitted respiratory and cardiac motion (Fig. 7). Fluid color sign intensity is inversely proportional to the viscosity of the effusion, while more complex and septated, the signal is less evident. Fluid color sign is helpful in distinguishing small pleural effusions (positive fluid color sign) from pleural thickening (absent fluid color sign) and has demonstrated 89.2% sensitivity and 100% specificity for detecting small pleural effusions [20].

Key indications for chest ultrasonography in neonatal and pediatric intensive care

Originally used to assess pleural effusions, guide thoracentesis, and evaluate opacified lung fields, ultrasonography has become an essential tool in the intensive care setting for examining the pulmonary parenchyma, particularly in critically ill patients. Expanding awareness and implementing this technique can help minimize unnecessary exposure to ionizing radiation, aligning with ALARA and Image Gently principles. This section outlines the key sonographic signs used in the evaluation of pleuropulmonary diseases, with a focus on critically ill patients.

Pneumothorax

Thoracic ultrasound is the most effective method for assessing pneumothorax, as it can be performed at the bedside and avoids unnecessary exposure to ionizing radiation. Therefore, it can be repeated as often as necessary, which is particularly useful in emergencies. Ultrasound can also detect small volumes of free air, making it a sensitive and specific method for detecting a pneumothorax.

The diagnosis of pneumothorax relies on the recognition of the presence or absence of the following four sonographic signs [21] (Supplementary Material 3):

- (a) *Absence of lung sliding sign* corresponds to the non-visualization of the pleural line motion during respiration [18]. It is important to note that several conditions besides pneumothorax can also result in the *absence of*

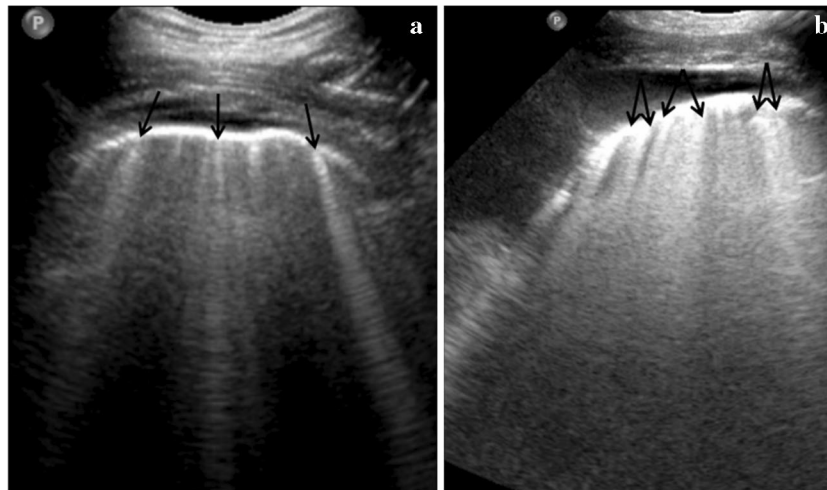


Fig. 3 B-lines. **a** The *B-lines* are vertically oriented artifactual hyperchoic lines that originate at the pleural line (*arrows*), extend toward the bottom portion of the screen, and move in synchrony with lung sliding. The presence of multiple B-lines, as seen here, suggests an interstitial lung process. **b** The *coalescent fan-shaped B-lines*

(*arrows*) correspond to the ground-glass pattern in CT. These images are transverse views of the posterior left midthoracic region of a 15-month-old male obtained using an 8–5 MHz microconvex transducer

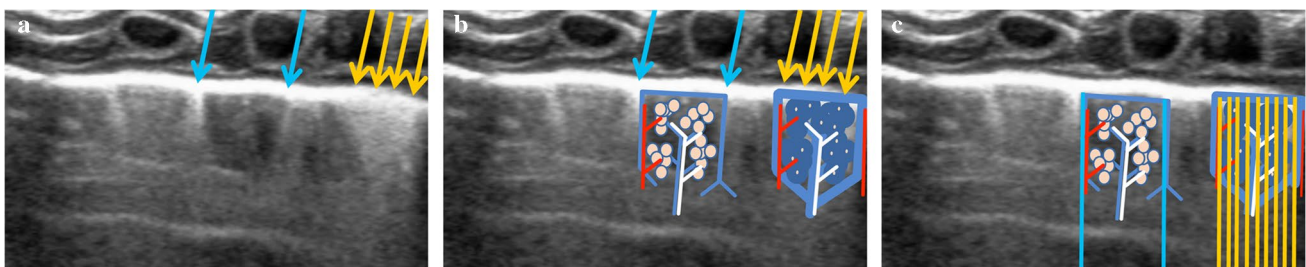


Fig. 4 Origin of well-defined and coalescent B-lines. Image of the anteroinferior region of the right lung in a newborn female, obtained using a high-frequency linear transducer (12 MHz), shows **(a)** well-defined B-lines (*blue arrows*) and coalescent B-lines (*yellow arrows*); **(b)** superimposed drawings clarifying the origin of these B-lines, with well-defined B-lines being artifacts resulting from the thickening

of the interlobular septa (*blue arrows*) and coalescent B-lines resulting from the thickened intralobular interstitium (*yellow arrows*) with some small intra-alveolar components; and **(c)** the positions of the well-defined B-lines (*blue lines*) and the coalescent B-lines (*parallel yellow lines*)

lung sliding sign, e.g., atelectasis, pleural adhesions, acute respiratory distress syndrome, phrenic nerve palsy, cardiopulmonary arrest, and apnea [17]. Additionally, the lung sliding sign may be absent in cases of *selective intubation* or *lung hyperinflation*, such as in the case of foreign body aspiration [22, 23]. Therefore, other signs must also be evaluated to ensure an accurate diagnosis.

- (b) *Absence of B-lines*—the visualization of B-lines strongly indicates the absence of pneumothorax (Fig. 8). However, the absence of B-lines does not necessarily indicate the presence of pneumothorax [17, 24].
- (c) *Presence of lung point*—the lung point represents the transition point between pneumothorax and preserved

lung sliding sign, indicating partial pneumothorax (Fig. 9). The lung point sign confirms partial pneumothorax with 100% specificity [17, 25]. However, this sign will be absent in the case of total lung collapse.

- (d) *Absence of lung pulse*—the visualization of *lung pulse* rules out pneumothorax in a consolidated lung.

The sonographic diagnosis of pneumothorax is made after carefully evaluating all four signs. Some authors still consider the *accentuation of A-lines* (see Fig. 8) as another sign of pneumothorax when associated with the previously mentioned findings.

M-mode can also demonstrate pneumothorax as a stratosphere/barcode sign representing the loss of the normal

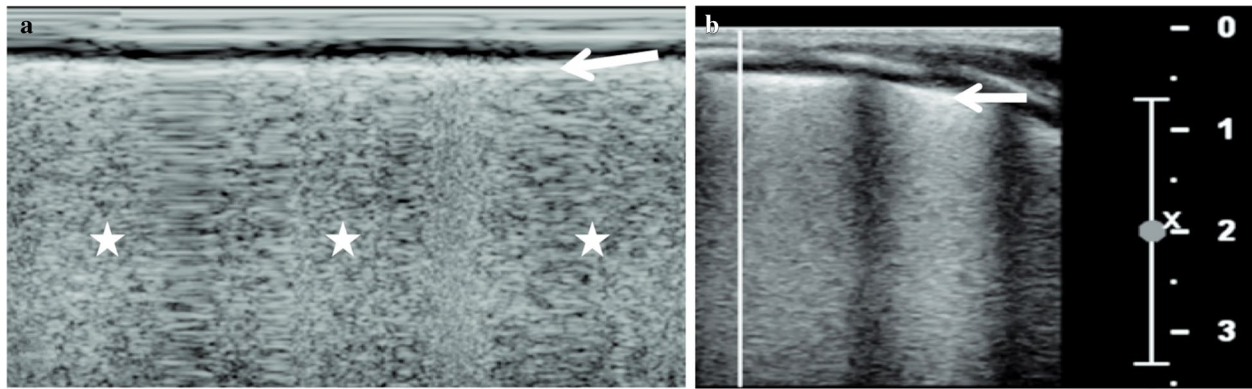


Fig. 5 Seashore sign. **a** The seashore sign is the pattern obtained with M-mode, where the normal lung sliding manifests as a sandy/granular pattern (*white stars*) below the hyperechoic line representing the pleural line (*white arrows* in **a** and **b**). **b** B-mode axial view through

the anterior region of the right mid-chest in a 1-year-8-month-old male obtained using a high-frequency linear transducer (12–5 MHz). The *white vertical line* indicates the level at which the M-mode image was obtained



Fig. 6 Tissue-like sign. The consolidated lung parenchyma (*black arrow*) shows a similar echogenicity to that of the liver (*star*) or spleen parenchyma. The diaphragm (*white arrow*) separates the consolidated lung from the liver. This image presents a longitudinal view of the right lung base of an 11-year-old male using a 5–2 MHz convex transducer

seashore sign (Fig. 9). Only the motionless chest wall components, represented by horizontal lines, are seen without the sandy component of lung motion due to pneumothorax.

Bedside chest ultrasonography in emergency cases, such as cardiac arrest or unstable patients, can significantly expedite diagnosis and facilitate appropriate therapeutic

measures, such as intubation and drainage of the pneumothorax [21].

Respiratory distress syndrome

Before 2010, the diagnosis of respiratory distress syndrome (RDS) was primarily achieved through chest radiography, with only a few studies using ultrasound as a diagnostic tool for this prevalent form of respiratory failure in preterm neonates [26–28].

A comparison between chest radiography and lung ultrasound in patients with RDS significantly favors lung ultrasound as a highly sensitive method for evaluating neonatal lungs [29].

RDS is characterized by alveolar collapse associated with interstitial edema due to insufficient surfactant production in premature newborns. The ultrasound examination shows an abnormal pleural line, absence of A-lines, and multiple coalescing B-lines due to interstitial or alveolar-interstitial edema, resulting in a sonographically white lung, with possible lung consolidation(s). After exogenous surfactant administration, this sonographic pathological pattern may not change immediately, as alveolar expansion occurs before the resolution of interstitial extravascular fluid. However, prompt improvement of pathological lung ultrasound findings has been reported [30]. Signs of improvement in lung aeration after surfactant treatment include (i) reduction in lung consolidation, (ii) reduction of B-lines, and (iii) appearance of A-lines (Fig. 10).

In 2008, Copetti et al. reported 100% sensitivity and specificity in diagnosing RDS with the presence of sonographic white lung (compact B-lines), pleural line abnormalities, and the absence of spared areas [28]. However, lung ultrasound findings depend on the grade/stage of RDS, which results in a broad spectrum of pathological patterns [12]. Because

Fig. 7 Color Doppler images depicting the fluid color sign in the pleural space fluid, resulting from respiratory motion and cardiac pulsation. These images were obtained by transverse scanning the left lateral basal hemithorax in a 12-year-old male using a high-frequency linear transducer (12–5 MHz). The study of fluid color sign aids in differentiating minimal pleural effusion from pleural thickening

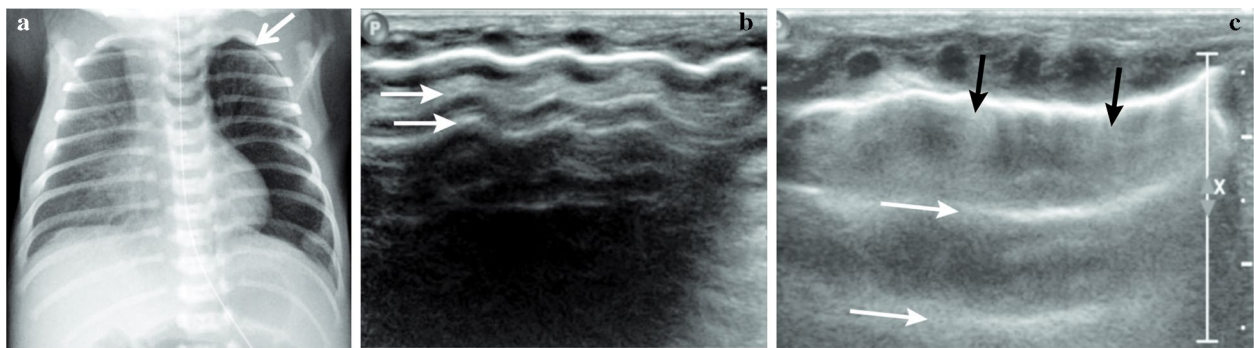
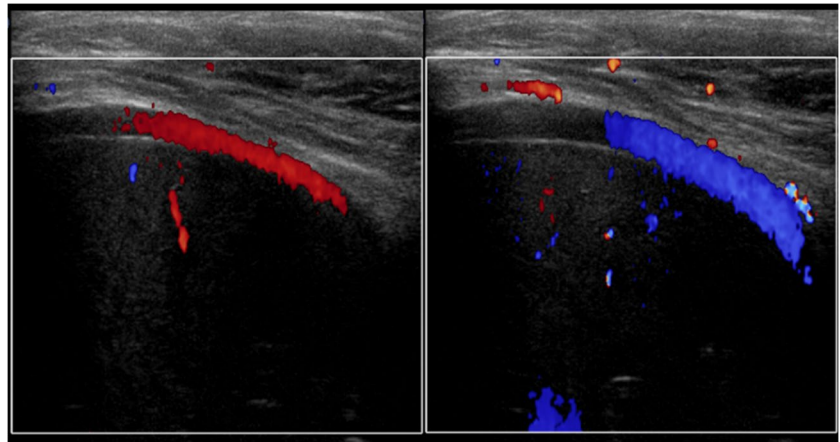


Fig. 8 A 3-day-old preterm male neonate, with *respiratory distress syndrome* and a small left pneumothorax. **a** The chest radiograph reveals, among other findings, a small left apical pneumothorax (arrow). **b** Transverse ultrasound image obtained with a 12–5 MHz high-frequency linear transducer of the left upper hemithorax shows

classic signs of pneumothorax, including accentuation of A-lines (arrows) and absence of B-lines. **c** The subsequent transverse scan of the right anterior mid-chest revealed normal appearing A-lines (white arrows), indicating improvement in the aeration pattern along with the presence of a few B-lines (black arrows)

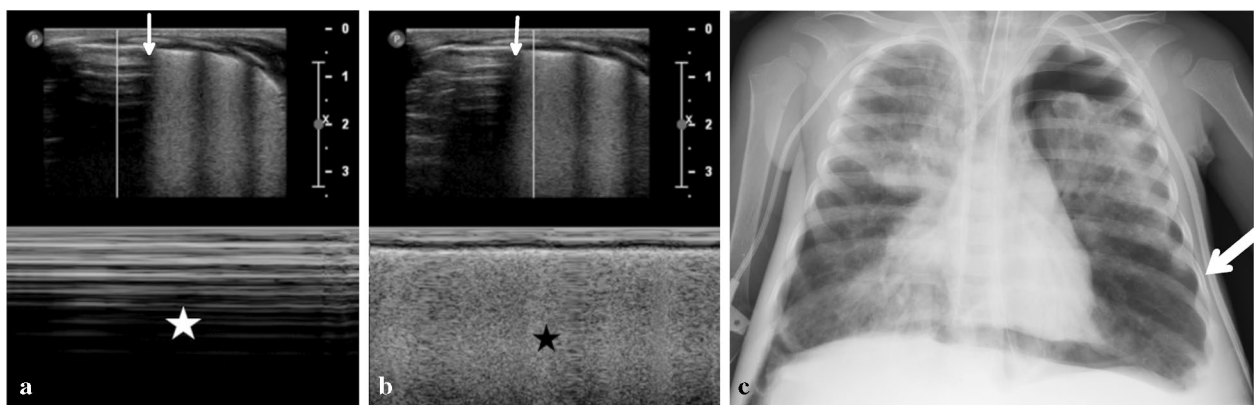


Fig. 9 Lung point and stratosphere/barcode sign of pneumothorax on M-mode ultrasound. **a** A longitudinal M-mode image of the left lateral lower hemithorax of a 20-month-old male using a high-frequency linear transducer (12–5 MHz) shows parallel horizontal lines (white star) representing the absence of lung motion due to the pneumothorax. Below this point, **(b)** one can observe the seashore sign (black

star) with the sandy pattern of lung sliding. The white vertical lines in the upper parts of the images in **(a)** and **(b)** show the level at which the M-mode images were obtained on B-mode. **c** Chest radiograph reveals a large left pneumothorax, with the white arrow indicating the location of the *lung point*, which is also indicated by the vertical white arrows on ultrasound images **(a)** and **(b)**

sonographic signs of interstitial edema occur before changes in PaO₂/FiO₂, lung ultrasound at birth can detect neonates with RDS before clinical deterioration, assisting in clinical decision-making for early surfactant administration.

The persistence of interstitial edema signs may indicate potential interlobular septal fibrosis and subsequent bronchopulmonary dysplasia [31]. Therefore, lung ultrasound is also helpful in monitoring treatment and prognosis.

Transient tachypnea of the newborn

In transient tachypnea of the newborn, lung ultrasound images reveal a “wet lung” appearance due to excessive bronchial secretions and incomplete absorption of fetal lung fluid. This condition is characterized by pulmonary capillary congestion with interstitial edema and is more prevalent in infants born via cesarean section, particularly those delivered before the onset of labor [32].

A typical finding of transient tachypnea of the newborn is the *double lung point*, which represents the interface between the upper lung fields with normal aeration (A-lines) and the basal lung fields that still exhibit interstitial edema (coalescent B-lines) (Fig. 11).

Until recently, the double lung point sign was thought to be specific to transient tachypnea of the newborn and considered its pathognomonic feature. However, recent extensive studies have shown that this sign is also seen in other conditions, such as during the recovery period of severe RDS, meconium aspiration syndrome, and pneumonia. The sensitivity for detecting transient tachypnea of the newborn ranges from 34.1% to 100%, with high specificity ranging from 94.8% to 100% [33, 34].

Meconium aspiration syndrome

In lung ultrasound, meconium aspiration syndrome manifests as subpleural consolidation with air bronchograms, varying amounts of B-lines, pleural abnormalities, and rarely pleural effusion. Therefore, distinguishing meconium aspiration syndrome from pneumonia can be challenging without clinical and laboratory correlation [11].

Consolidation

When the alveolar air is replaced by fluid, the lung consolidates. On ultrasound, the consolidated lung appears as a

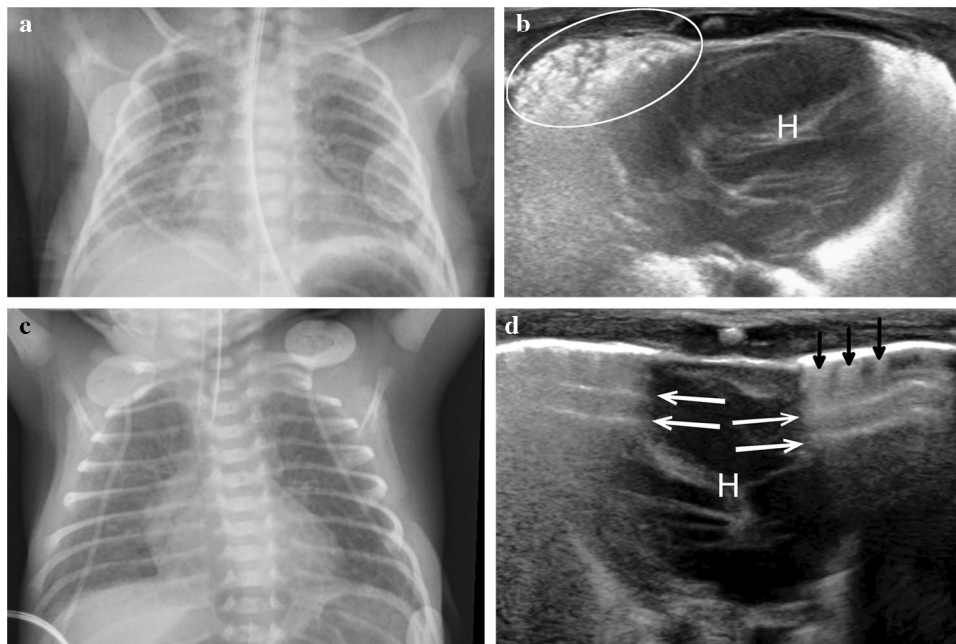


Fig. 10 Premature female newborn with RDS at the 4th hour of life. **a** Chest radiograph depicts typical findings of RDS, including hypoexpanded lungs with fine reticulation and scattered hazy opacities. **b** The transverse lung ultrasound image obtained using a high-frequency linear transducer (12–5 MHz), in the precordial region (*H* is the heart), shows an irregular pleural line, absence of A-lines, and subpleural lung consolidation with air bronchograms (*encircled*

area). **c** Three days later, after surfactant administration, an improvement in the lung aeration pattern was observed with better lung expansion on chest radiograph. **d** Lung ultrasound performed later the same day confirmed the chest radiographic findings, showing improvement in lung aeration with the appearance of some A-lines (*white arrows*) and a few B-lines (*black arrows*), proving the effectiveness of treatment

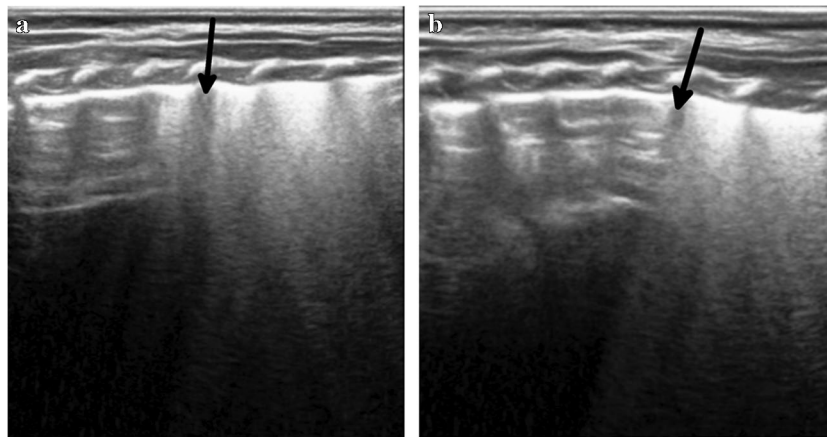


Fig. 11 Full-term newborn female with *respiratory distress*. **a** Longitudinal image of the right mid-lateral chest using a high-frequency linear transducer (12–5 MHz) and **(b)** longitudinal scan of the left mid-lateral chest also using a high-frequency linear transducer (12–5

MHz). Both images (**a** and **b**) show the double lung point (*black arrows*), the transition point between the upper lung fields with normal aeration (A-lines), and the basal lung fields still showing interstitial edema (coalescent B-lines, white lung)

solid tissue similar to the liver, hence called *hepatization* or *tissue-like sign* (see Fig. 6), depending on the degree of air loss replaced by fluid.

Pneumonia

The detection of pneumonia is a well-known application of lung ultrasound. However, distinguishing between bacterial and viral pneumonia presents a challenge. Some authors have claimed that a consolidative process larger than 20 mm favors bacterial pneumonia. A single focal area of consolidation is also suggestive of bacterial pneumonia. In contrast, multiple small consolidations suggest viral pneumonia [35, 36]. B-lines often accompany lung consolidations in both bacterial and viral pneumonia. However, the most significant limitation of all studies is the lack of a gold-standard diagnostic test.

Common ultrasound findings of viral pneumonia include multifocal, coalescent B-lines (ground-glass pattern), multifocal small subpleural consolidations, irregularity and thickening of the pleural line, while pleural effusion is rare (Fig. 12).

In SARS-CoV-2 pneumonia, lung ultrasound primarily shows multifocal separate and coalescent B-lines (ground-glass pattern), as well as multifocal small subpleural consolidations (predominantly < 1 cm), and irregularity and thickening of the pleural line, with pleural effusion being rare (Fig. 13) [37, 38].

In the congestive stage of pneumonia, a consolidated lung exhibits an echotexture similar to that of the liver or spleen by ultrasound (i.e., hepatization or tissue-like sign), with air bronchograms presenting as echogenic branching opacities (Fig. 14) [39]. The dynamic air bronchogram sign can be seen in the dynamic, real-time study in these cases of pneumonia,

where one can observe the air movement inside the bronchi, enabling differentiation with cases of resorptive atelectasis, with a specificity of 94% and a positive predictive value of 97% (Supplementary Material 4) [40]. However, fluid bronchograms due to fluid or mucoid content within the bronchi can also be observed along with hypoechoic branching patterns.

Color Doppler can help distinguish pulmonary vessels from fluid-filled bronchi within the consolidated lung parenchyma, showing branching patterns [41, 42]. Gussinye and Serres correlated the B-mode and color Doppler patterns of pneumonic foci assessed by sonography with the duration of hospitalization [43]. These patterns were classified as (i) well-vascularized (Fig. 14), (ii) non-necrotizing hypovascularized (Fig. 15), or (iii) necrotizing non-vascularized, avascularized (Fig. 16, and Supplementary Materials 5 and 6) and correlated with the length of stay of 6 days, 9 days, and 21 days, respectively. Lai et al. proposed a similar procedure, with different nomenclature, to describe the degree of vascularization for lung parenchyma through qualitative Doppler mode, categorizing perfusion into three stages, (i) *normal* – showing the homogeneous distribution of vascularity; (ii) *decreased* – less than 50% area of vascularity; or (iii) *poor* – with no recognizable vascularization [44]. Any suspicion of hypovascularity of the consolidated lung necessitates frequent lung ultrasound follow-ups to detect early stages of necrotic lung development.

Literature reviews and meta-analyses have identified four clinical signs most frequently used in lung ultrasound screening criteria for children with pneumonia: lung consolidation, air/fluid bronchograms, abnormal pleural line, and pleural effusion [45–49]. These studies have also reported that lung ultrasounds pooled sensitivity for detecting pneumonia ranges from 93% to 95%, with a specificity ranging from 90% to 96% [50].

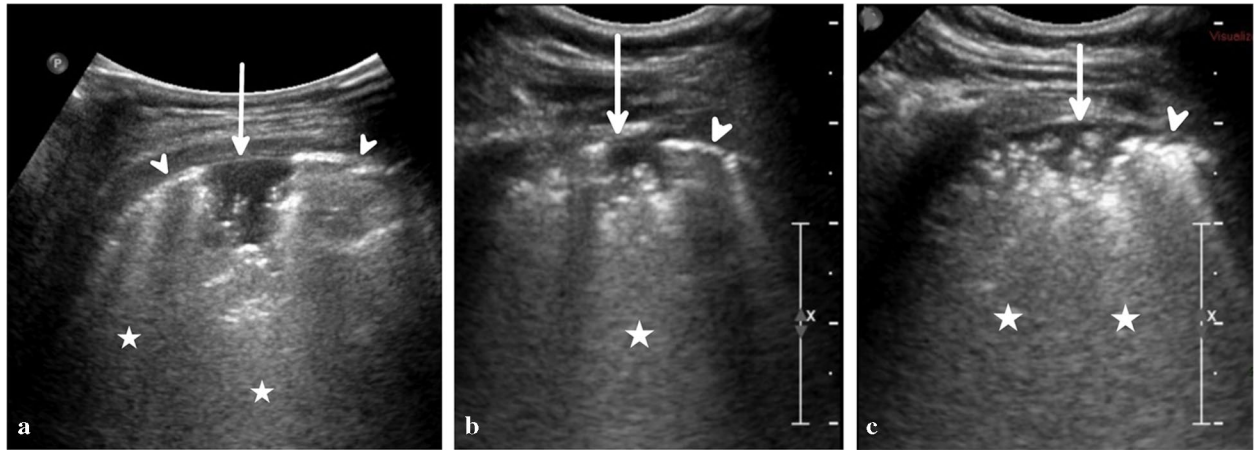
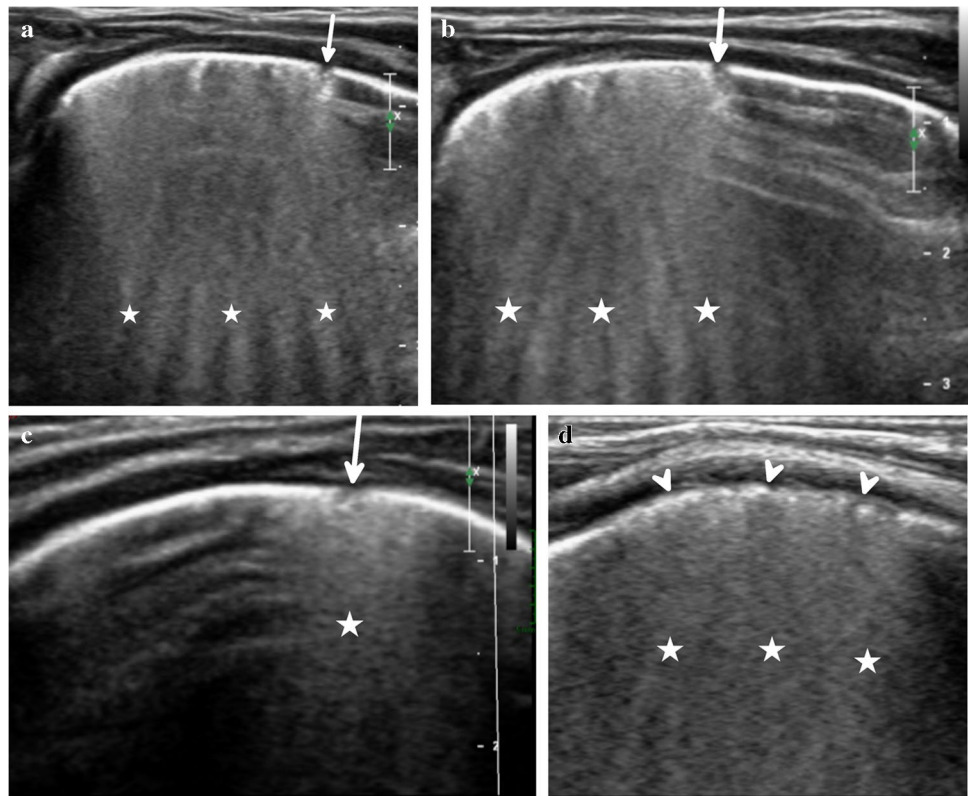


Fig. 12 Respiratory syncytial virus bronchiolitis in a 3-month-old female admitted to the neonatal intensive care unit requiring mechanical ventilation. **a, b, c** All ultrasound images scanned with a microconvex 8–5 MHz transducer show multifocal subpleural consol-

idations (*arrows* in **a, b,** and **c**) and pleural line irregularities (*arrowheads* in **a, b,** and **c**) bilaterally in the posteroinferior lung fields. Coalescent B-lines are also present (*stars* in **a, b,** and **c**)

Fig. 13 SARS-CoV-2 pneumonia in a 7-day-old male. All ultrasound images obtained with a 12–5 MHz linear transducer from (**a, b, d**) the right and (**c**) left hemithoraces in the posteroinferior lung fields show multifocal small subpleural consolidation (*arrows* in **a, b,** and **c**) and irregularity of the pleural line (*arrowheads* in **d**), as well as coalescent B-lines in all images (*stars*)



Pulmonary complications of infections

Some pneumonia cases may evolve into lung necrosis depending on the degree of virulence of the pathogens and the host’s immune status.

As most pneumonic processes reach the pleural surface, it is relatively easy to detect consolidated lung parenchyma

by sonography and the area(s) of necrosis within the lung as hypoechoic areas without a color Doppler signal. Cavitation or abscesses can also be detected within the consolidated lung. In cases of cavitation, a circumscribed hyperechoic area is observed, indicating the presence of air. Conversely, pulmonary abscesses appear as round hypoechoic areas, reflecting fluid content (Figs. 17 and 18).

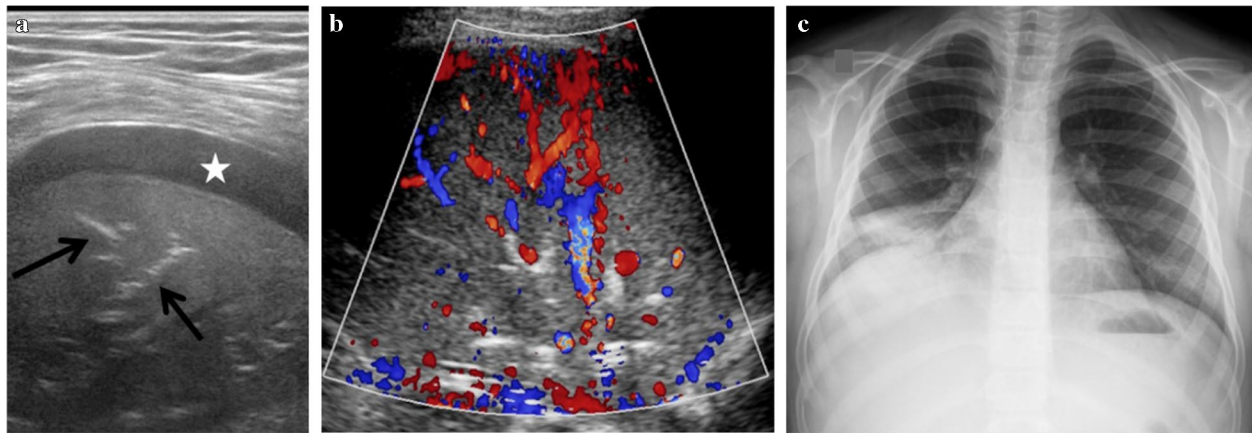


Fig. 14 Well-vascularized pneumonia in a 7-year-old male. **a** Transverse view of the right chest base obtained with a high-frequency (12–5 MHz) transducer shows lung consolidation with the tissue-like sign, air bronchograms seen as hyperechoic branching opacities (*black arrows*), and anechoic pleural effusion (*white star*). **b** The con-

solidation is well-vascularized on color Doppler. **c** Chest radiography shows opacification of the right lung base and obliteration of the right costophrenic angle (see also the companion Supplementary Material 4 for this case)

Fig. 15 Non-necrotizing hypovascularized pneumonia in a 4-year-old female. **a** Color Doppler ultrasound with a linear high-frequency 12–5 MHz transducer shows hypovascularized pneumonia without necrotizing foci. **b** The chest radiograph shows the focus of pneumonia in the left lower lung field

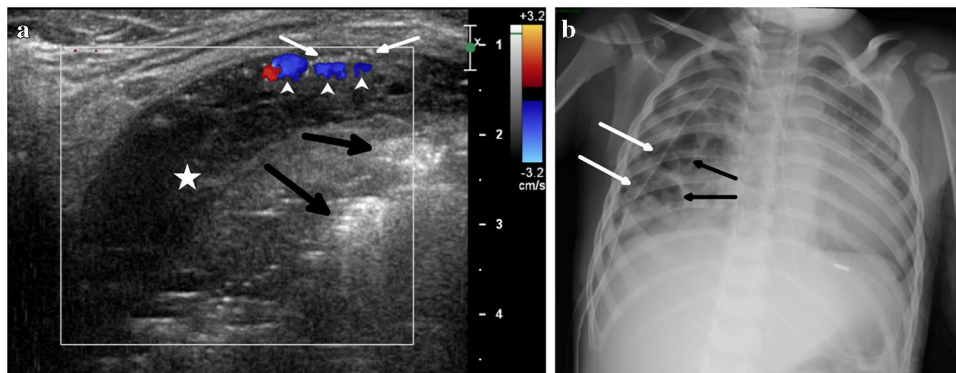
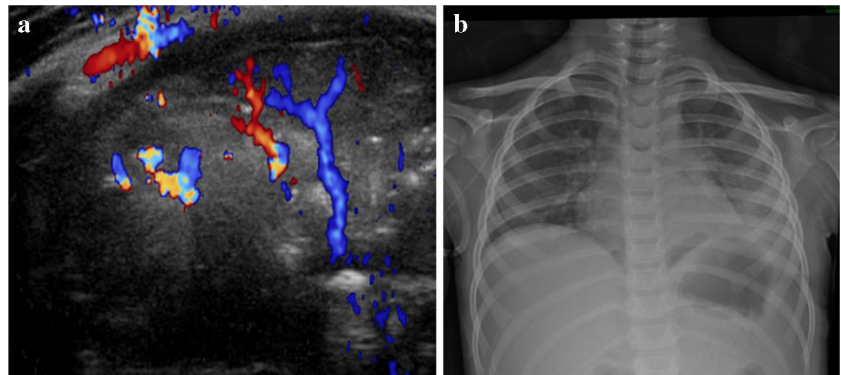


Fig. 16 Necrotizing non-vascularized pneumonia in a 2-year-old girl. **a** Color Doppler ultrasound of the right lung base obtained with a linear high-frequency 12–5 MHz transducer shows a marked decrease in vascularization with a pattern of necrotizing pneumonia, which is usually associated with a less favorable prognosis and a prolonged hospital stay. Rounded, hyperechoic foci represent air-filled cavities within the lung parenchyma (*black arrows*). There are a few signs on color Doppler study (*white arrowheads*) in the periphery of the pleural space containing organized empyema (*white star*). The minimal

fluid color sign indicates the presence of an organized and complex empyema. This weak Doppler signal appears only in the area with the larger fluid component. Some air bubbles (*white arrows*) can also be observed in the same area due to the presence of the chest tube on this side (*white arrows* in **b**). **b** Chest radiograph shows scattered opacities with small lucent areas (*black arrows*) representing air-filled cavities corresponding to the ultrasound findings shown in (**a**, *black arrows*) (see also the companion Supplementary Material 6 for this case)

Standardized lung ultrasound reports are recommended for patients with pneumonia or complicated pneumonia to facilitate follow-up and enhance report clarity for clinicians (Table 1).

Atelectasis

There are two main types of atelectasis [51, 52]:

- (a) *Compressive* – most frequently caused by voluminous pleural effusion that compresses the lung. The triangular-shaped atelectatic segment moves in the pleural fluid like a waving hand (Fig. 19).
- (b) *Obstructive*, which occurs when foreign objects or mucus plugs lodged in one of the major bronchi obstruct the airway. The trapped air in the distal segment is slowly absorbed (Fig. 20).

The sonographic characteristics of obstructive atelectasis are strikingly similar to those of pneumonia. Both conditions show hepatization of the lung parenchyma and air bronchograms, but, in pneumonia, air movement within the bronchi can be observed (dynamic air bronchogram).

Pleural effusion

Ultrasonography is the preferred method for evaluating pleural effusion and guiding thoracentesis. The evaluation of pleural effusions can be initiated with B-mode, employing lower frequency transducers such as the 8–5 MHz microconvex or the 9–4 MHz convex transducer, which is particularly useful for assessing and estimating the volume of the effusion. Subsequent assessment with a 12 MHz high-frequency transducer can provide a more

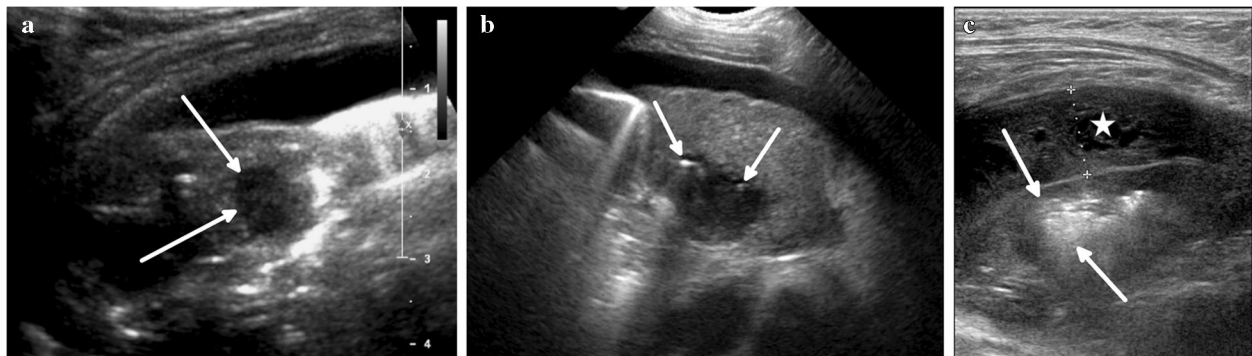


Fig. 17 Different stages of necrotizing pneumonia in three distinct patients. **a** An initial focus of liquefaction in the lung parenchyma, which on ultrasound using a convex transducer (9–4 MHz) appears as a circumscribed hypoechoic area (arrows) within the consolidated/hepatized lung parenchyma in a 3-month-old female. **b** An area of lung necrosis containing tiny gaseous hyperechoic foci (arrows) in a 1-year-old female patient, indicating a more advanced stage of

necrotizing pneumonia compared to the patient shown in (a). **c** With the progression of necrotizing pneumonia, cavitations are found, which appear on ultrasound as rounded images filled with gaseous hyperechoic contents (arrows). This image was obtained with a high-frequency linear transducer (12–5 MHz), in a 2-year-old female with necrotizing pneumonia with associated organizing empyema (star)

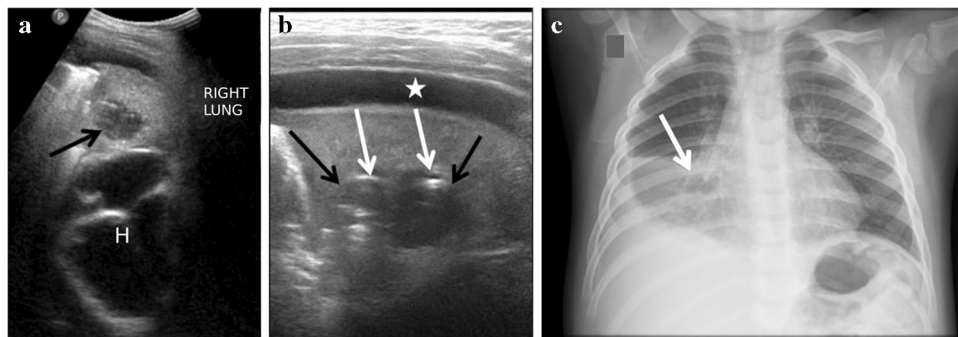


Fig. 18 Necrotizing pneumonia in a 1-year-old girl. **a, b** Oblique views of the right mid chest were obtained (a) with a convex transducer (9–4 MHz) and (b) with a high-frequency linear transducer (12–5 MHz). These images show focal hypoechoic rounded areas within the consolidated middle lobe consistent with necrotic areas

(black arrows in a and b) in necrotizing pneumonia (white arrow in c). Additionally, note the presence of hyperechoic foci within these cavitations, which correspond to gaseous foci (white arrows). There is an associated parapneumonic, anechoic pleural effusion (star). H in (a) indicates the heart

Table 1 What should be reported on lung ultrasound in cases of pneumonia?

1	Is there pleural effusion? If present, report the estimated volume or thickness	Yes no
2	Characterize the pleural effusion	Anechoic hypoechoic with or without debris, septations
3	If present, characterize pleural empyema	Exudative fibrinopurulent chronic organizing
4	Lung parenchyma appearance	Homogeneous heterogeneous
5	Are there any signs of lung parenchyma necrosis?	Yes no
6	Vascularization of the lung parenchyma in the consolidated area by color Doppler sonography	Well-vascularized hypovascular avascular



Fig. 19 Compressive atelectasis in a 2-year-old male. This longitudinal ultrasound image from the right lateral chest base obtained using a microconvex (8–5 MHz) transducer shows a massive pleural effusion (*star*) compressing the pulmonary parenchyma, resulting in significant atelectasis (*arrows*)

detailed characterization of the fluid's quality, facilitating differentiation between anechoic fluid and the presence of thicker components or fibrin septations. While B-mode evaluation is often sufficient, it is crucial to note that in cases where the diagnosis remains uncertain, particularly to differentiate between pleural effusion and pleural thickening, the use of the Doppler fluid color sign, as previously described, can provide additional diagnostic value. Although high-resolution devices and transducers have rendered B-mode sufficient for this purpose, not all facilities possess such resources; therefore, the fluid color sign obtained with color Doppler remains extremely beneficial. To enhance the efficacy of this signal, the use of 8–5 MHz microconvex transducers or even 9–4 MHz convex transducers is recommended. Additionally, lowering the pulse-repetition frequency and increasing the gain of the color mode can optimize the fluid color sign performance. The appearance of pleural effusion on chest ultrasound varies based on the nature and components of the effusion, manifesting as anechoic or hyperechoic and may present thin or thick septations. In parapneumonic pleural effusions, the following aspects can be observed (Fig. 21) [53]:

- (a) *Anechoic*—transudates are almost invariably anechoic. Exudates may also appear anechoic. The fluid color sign is present in both cases.

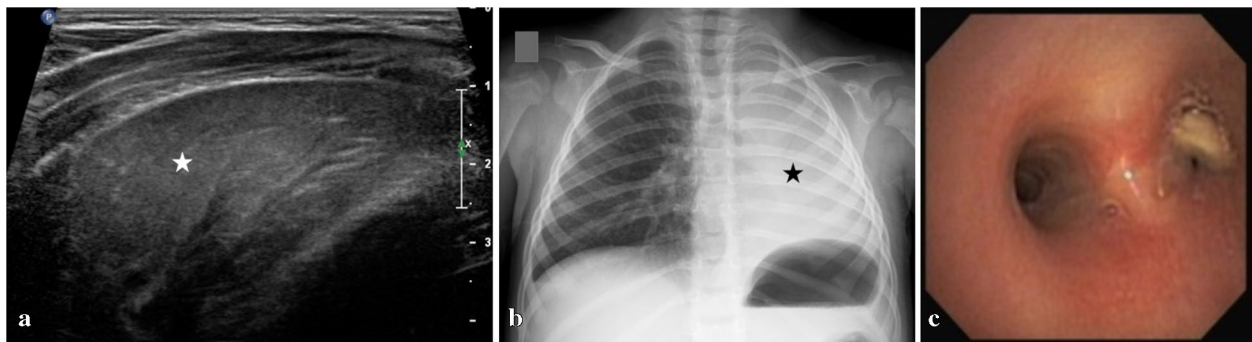


Fig. 20 Obstructive atelectasis in a 2-year-old female due to peanut aspiration. **a** Ultrasound of the left hemithorax obtained with a high-frequency linear transducer (12–5 MHz) shows a pattern similar to pneumonia, with a tissue-like sign (*white star*) but without air

bronchograms. **b** Chest radiograph shows complete opacification of the left hemithorax (*black star*) with mediastinal shift to the left. **c** Bronchoscopy image shows a peanut obstructing the left mainstem bronchus

- (b) *Complex nonseptate* corresponds to the exudative stage of pleural empyema, visualized as echogenic, with thick fluid (empyema is not distinguishable from hemothorax). The fluid color sign is present.
- (c) *Complex septate* corresponds to the fibrinopurulent stage, characterized by limited lung expansion (Supplementary Material 7). The fluid color sign is weakly present.
- (d) *Echogenic* depicts a chronic organizing stage (Supplementary Material 8) with thick, non-fluctuating exudate, pleural thickening, thick septations, and a trapped lung (lung sliding is often reduced or absent). The fluid color sign is absent.

Prompt recognition of a complicated pleural effusion is critical. Early thoracoscopy with the injection of fibrinolytic drugs offers numerous benefits in managing pleural empyema in pediatric patients. The injection of fibrinolytic drugs during thoracoscopy reduces morbidity and mortality, promotes earlier chest tube removal, shortens hospitalization, and improves the response to antibiotic therapy [54, 55].

The role of ultrasound in evaluating pleural effusion extends beyond mere quantification. A qualitative assessment of the effusion is imperative to identify incipient signs of empyema, ascertain the presence of fibrin septations, and

evaluate the organization of pleural effusion with pulmonary incarceration.

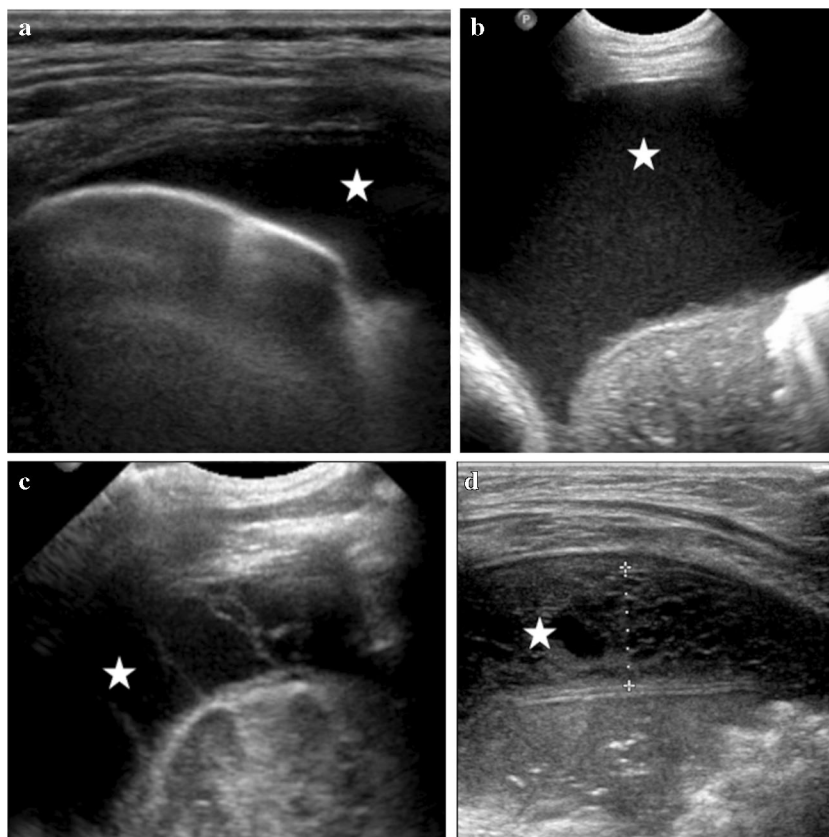
Upon detecting fibrin septations, it is essential to notify a pediatrician or thoracic surgeon promptly. This notification is crucial for performing a video thoracoscopy with fibrinolytic drug injection, which is known to yield favorable patient outcomes and reduce hospital stays [54, 55].

Lung ultrasonography to guide PEEP-induced lung recruitment

A novel application of lung ultrasound is the real-time guidance of lung recruitment induced by positive end-expiratory pressure at the bedside, a procedure that would otherwise require the transportation of the patient to the CT unit and the mobilization of the entire multidisciplinary team to support the critically ill patient. This procedure was first performed in adults by Bouhemad et al. in 2011 [56]. Lung ultrasound is used to assess alveolar recruitment based on airborne artifacts. Four patterns of lung aeration can be identified by lung ultrasound [56] (see Fig. 22):

- (a) *Pattern 1*—normal pattern—characterized by the presence of A-lines;

Fig. 21 Four sonographic patterns of pleural effusion from different patients (*white stars* indicate pleural effusions): (a) *anechoic* pleural effusion, corresponding to transudate in a 1-year-old female; (b) *complex nonseptate* pleural effusion in a 2-year-old male, indicating an exudative stage of pleural empyema; (c) *complex septate* pleural effusion in a 2-year-old male child, observed in the fibrinopurulent stage of pleural empyema; and (d) *echogenic/heterogeneous* pleural effusion with *thick septations*, indicating proliferation of fibroblasts, corresponding to the chronic organizing stage of pleural empyema, in a 2-year-old female. The images (a) and (d) were obtained with a high-frequency (12–5 MHz) linear transducer, while the images (b) and (c) were obtained with a microconvex (8–5 MHz) transducer



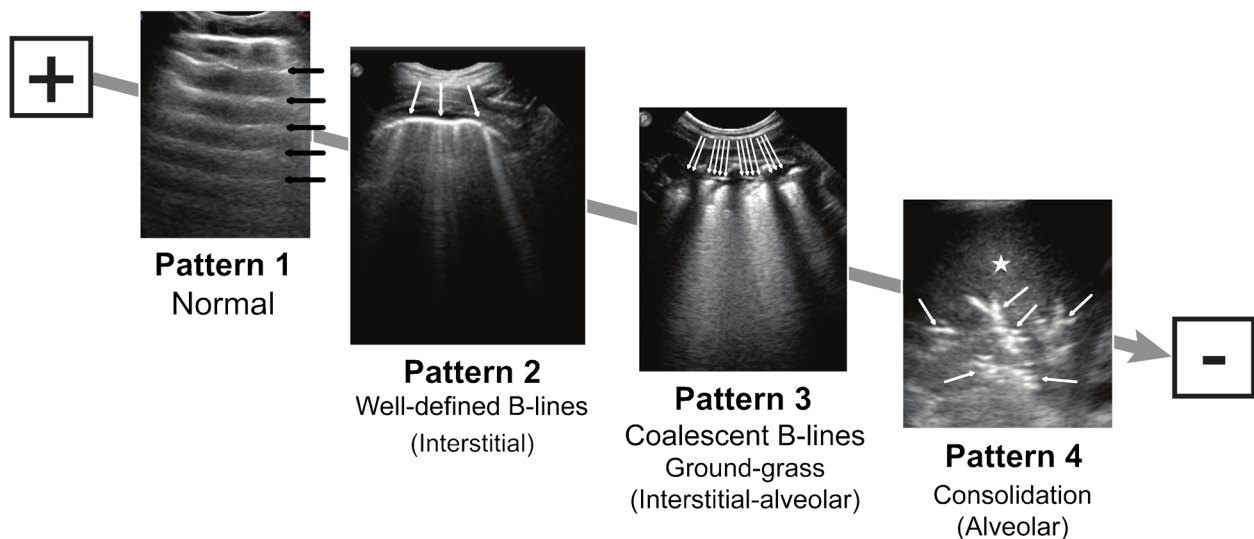


Fig. 22 Ultrasound patterns of lung aeration. The sequence of lung ultrasonographic patterns shows lung images with progressive loss of aeration from left to right. *Pattern 1* corresponds to normal aeration with multiple A-lines (*black arrows*). *Pattern 2* is characterized by multiple irregularly spaced B-lines (well-defined B-lines, *white arrows*) with a moderate reduction in lung aeration. With the further loss of aeration due to pulmonary edema or confluent bronchopneumonia with partial filling of the alveolar spaces, *Pattern 3* is reached,

which evolves into marked coalescent B-lines (*white arrows*), forming the “ground-glass” areas on CT. *Pattern 4* shows a complete loss of aeration with lung consolidation with a tissue-like sign (*white star*) and air bronchograms (*white arrows*). The images depicting aeration *Patterns 1, 2, and 3* were obtained from the same 15-month-old male in different lung areas, while the image of *Pattern 4* was obtained from a 5-year-old female

- (b) *Pattern 2*—moderate reduction in lung aeration due to interstitial disease—characterized by the presence of multiple well-defined B-lines or irregularly spaced B-lines;
- (c) *Pattern 3*—severe reduction in lung aeration due to partial filling of alveolar spaces by pulmonary edema or confluent bronchopneumonia—marked by the presence of coalescent B-lines, corresponding to ground-glass areas on chest CT; and
- (d) *Pattern 4*—complete loss of lung aeration with persisting aeration of distal bronchioles—corresponds to lung consolidation with dynamic bronchograms.

Careful identification of lung aeration patterns while performing lung recruitment procedures guided by ultrasound is essential for controlling or monitoring the degree of lung reaeration. This procedure aims to transiently increase transpulmonary pressure, reopen collapsed alveoli, and recruit additional alveolar areas for gas exchange. At the same time, lung ultrasound monitors the change in aeration status in real time [57].

Conclusions

Lung ultrasound has broad applicability in neonatal and pediatric patients. Its well-documented advantages over other imaging modalities include the absence of ionizing

radiation, noninvasiveness, and portability for bedside examination. These features are particularly important in critically ill patients with alveolar-interstitial processes, complicated pneumonia, lung consolidation, pneumothorax, and pleural effusion, enabling active real-time evaluation. Nevertheless, lung ultrasound has several limitations, including operator dependency and restricted visualization due to the location of pathological entities (e.g., perihilar or mediastinal lung surfaces) or gas interposition, as seen in pneumothorax and subcutaneous emphysema. Despite these limitations, the advantages of lung ultrasound in neonatology and pediatrics remain substantial, and it has been utilized to diagnose and monitor a variety of chest diseases. Over the past 5 to 6 years, significant efforts have been made to expand the role of lung ultrasound in neonatal and pediatric intensive care units.

Supplementary Information The online version contains supplementary material available at <https://doi.org/10.1007/s00247-025-06300-8>.

Acknowledgements We sincerely thank the editor and reviewers for their insightful feedback, which significantly improved the manuscript.

Author contribution Y.T.S. and J.L. wrote the initial draft of the manuscript. Y.T.S. prepared the figures. Y.T.S., F.G.O. and M.W.M. gathered and selected the case. All authors reviewed the manuscript. Y.T.S. and M.A.R. prepared and narrated the videos.

Data availability No datasets were generated or analysed during the current study.

Declarations

Conflicts of interest The authors declare no competing interests.

Ethics approval In compliance with ethical standards.

References

- Lichtenstein DA (2005) Lung ultrasound in the critically ill. *Clin Intensive Care* 16:79–87
- Lichtenstein DA, Mézière G, Biderman P et al (1997) The comet-tail artifact. *Am J Respir Crit Care Med* 156:1640–1646
- Shelmerdine SC, Lovrenski J, Caro-Domínguez P et al (2020) Coronavirus Disease 2019 (COVID-19) in children: a systematic review of imaging findings. *Pediatr Radiol* 50:1217–1230
- Sönmez LO, Katipoğlu B, Vatansav H et al (2021) The impact of lung ultrasound on coronavirus disease 2019 pneumonia suspected patients admitted to emergency departments. *Ultrasound Q* 37:261–266
- La Regina DP, Pepino D, Nenna R et al (2022) Pediatric COVID-19 follow-up with lung ultrasound: a prospective cohort study. *Diagnostics* 12:2202
- Goske MJ, Applegate KE, Boylan J et al (2008) The image gently campaign: working together to change practice. *Am J Roentgenol* 190:273–274
- Joshi P, Vasishtha A, Gupta M (2019) Ultrasound of the pediatric chest. *Br J Radiol* 92:20190058
- Jaworska J, Buda N, Ciuca IM et al (2021) Ultrasound of the pleura in children, WFUMB review paper. *Med Ultrason* 23:339–347
- Bhalla D, Naranje P, Jana M, Bhalla AS (2022) Pediatric lung ultrasonography: current perspectives. *Pediatr Radiol* 52:2038–2050
- Liu J, Guo G, Kurepa D et al (2022) Specification and guideline for technical aspects and scanning parameter settings of neonatal lung ultrasound examination. *J Matern Fetal Neonatal Med* 35:1003–1016
- Liu J, Copetti R, Sorantin E et al (2019) Protocol and guidelines for point-of-care lung ultrasound in diagnosing neonatal pulmonary diseases based on international expert consensus. *J Vis Exp* 145:1–20
- Lovrenski J (2020) Pediatric lung ultrasound — pros and potentials. *Pediatr Radiol* 50:306–313
- Lichtenstein D, Malbrain ML (2015) Critical care ultrasound in cardiac arrest. Technological requirements for performing the sesame-protocol — a holistic approach. *Anaesthesiol Intensive Ther* 47:471–481
- Tomà P (2020) Lung ultrasound in pediatric radiology - cons. *Pediatr Radiol* 50:314–320
- Gargani L, Bruni C, Romei C et al (2020) Prognostic value of lung ultrasound B-lines in systemic sclerosis. *Chest* 158:1515–1525
- Lichtenstein DA, Lascols N, Prin S, Mézière G (2003) The “lung pulse”: an early ultrasound sign of complete atelectasis. *Intensive Care Med* 29:2187–2192
- Lichtenstein DA (2014) Lung ultrasound in the critically ill. *Ann Intensive Care* 4:1
- Lichtenstein DA (2007) Ultrasound in the management of thoracic disease. *Crit Care Med* 35:S250
- Lichtenstein DA, Lascols N, Mézière G, Gepner A (2004) Ultrasound diagnosis of alveolar consolidation in the critically ill. *Intensive Care Med* 30:276–281
- Wu RG, Yang PC, Kuo SH, Luh KT (1995) “Fluid color” sign: a useful indicator for discrimination between pleural thickening and pleural effusion. *J Ultrasound Med* 14:767–769
- Volpicelli G (2011) Sonographic diagnosis of pneumothorax. *Intensive Care Med* 37:224–232
- Lovrenski J, Dautović GV, Lovrenski A (2019) Reduced or absent “lung sliding” - a novel lung ultrasound sign of pediatric foreign body aspiration. *J Ultrasound Med* 38:3079–3082
- Fernández LR, Hernández RG, Guerediaga IS et al (2022) Usefulness of lung ultrasound in the diagnosis and follow-up of respiratory diseases in neonates. *An Pediatr (Barc)* 96:252.e1–252.e13
- Lichtenstein D, Mézière G, Biderman P, Gepner A (1999) The comet-tail artifact: an ultrasound sign ruling out pneumothorax. *Intensive Care Med* 25:383–388
- Lichtenstein DA, Mézière G, Biderman P, Gepner A (2000) The “lung point”: an ultrasound sign specific to pneumothorax. *Intensive Care Med* 26:1434–1440
- Avni EF, Braude P, Pardou A, Matos C (1990) Hyaline membrane disease in the newborn: diagnosis by ultrasound. *Pediatr Radiol* 20:143–146
- Bober K, Swietliński J (2006) Diagnostic utility of ultrasonography for respiratory distress syndrome in neonates. *Med Sci Monit* 12:CR440–CR446. URL <https://medscimonit.com/abstract/index/idArt/459200>
- Copetti R, Cattarossi L, Macagno F et al (2008) Lung ultrasound in respiratory distress syndrome: a useful tool for early diagnosis. *Neonatology* 94:52–59
- Sefic Pasic I, Riera Soler L, Vazquez Mendez E, Castillo Salinas F (2022) Comparison between lung ultrasonography and chest x-ray in the evaluation of neonatal respiratory distress syndrome. *J Ultrasound* 26:435–448
- Lovrenski J, Sorantin E, Stojanovic S et al (2015) Evaluation of surfactant replacement therapy effects: a new potential role of lung ultrasound. *Srp Arh Celok Lek* 143:669–675
- Pieper CH, Smith J, Brand EJ (2004) The value of ultrasound examination of the lungs in predicting bronchopulmonary dysplasia. *Pediatr Radiol* 34:227–231
- Morrison JJ, Rennie JM, Milton PJ (1995) Neonatal respiratory morbidity and mode of delivery at term: influence of timing of elective caesarean section. *BJOG* 102:101–106
- Liu J, Chen XX, Li XW et al (2016) Lung ultrasonography to diagnose transient tachypnea of the newborn. *Chest* 149:1269–1275
- Raimondi F, Yousef N, Rodriguez Fanjul J et al (2019) A multicenter lung ultrasound study on transient tachypnea of the neonate. *Neonatology* 115:263–268
- Berce V, Tomazin M, Gorenjak M et al (2019) The usefulness of lung ultrasound for the aetiological diagnosis of community-acquired pneumonia in children. *Sci Rep* 9:17957
- Malla D, Rathi V, Gomber S, Upreti L (2021) Can lung ultrasound differentiate between bacterial and viral pneumonia in children? *JCU* 49:91–100
- Caro-Dominguez P, Shelmerdine SC, Toso S et al (2020) Thoracic imaging of coronavirus disease 2019 (COVID-19) in children: a series of 91 cases. *Pediatr Radiol* 50:1354–1368
- Guitart C, Suárez R, Girona M et al (2021) Lung ultrasound findings in pediatric patients with COVID-19. *Eur J Pediatr* 180:1117–1123
- Görg C, Seifart U, Görg K, Zugmaier G (2003) Color Doppler sonographic mapping of pulmonary lesions. *J Ultrasound Med* 22:1033–1039
- Lichtenstein D, Mézière G, Seitz J (2009) The dynamic air bronchogram: a lung ultrasound sign of alveolar consolidation ruling out atelectasis. *Chest* 135:1421–1425
- Acunas B, Celik L, Acunas A (1989) Chest sonography: differentiation of pulmonary consolidation from pleural disease. *Acta Radiol* 30:273–275

42. Targhetta R, Chavagneux R, Bourgeois JM et al (1992) Sonographic approach to diagnosing pulmonary consolidation. *J Ultrasound Med* 11:667–672
43. Gussinye P, Serres X (2002) Ecografía torácica como prueba pronóstica en neumonías que requieren ingreso. *An Pediatr (Barc)* 56:132–134
44. Lai SH, Wong KS, Liao SL (2015) Value of lung ultrasonography in the diagnosis and outcome prediction of pediatric community-acquired pneumonia with necrotizing change. *PLoS ONE* 10:e0130082
45. Pereda MA, Chavez MA, Hooper-Miele CC et al (2015) Lung ultrasound for the diagnosis of pneumonia in children: a meta-analysis. *Pediatrics* 135:714–722
46. Xin H, Li J, Hu HY (2018) Is lung ultrasound useful for diagnosing pneumonia in children?: a meta-analysis and systematic review. *Ultrasound Q* 34:3–10
47. Yan JH, Yu N, Wang YH et al (2020) Lung ultrasound vs chest radiography in the diagnosis of children pneumonia: systematic evidence. *Medicine* 99:e23671
48. Dong Z, Shen C, Tang J et al (2023) Accuracy of thoracic ultrasonography for the diagnosis of pediatric pneumonia: a systematic review and meta-analysis. *Diagnostics* 13:3457
49. Yang Y, Wu Y, Zhao W (2024) Comparison of lung ultrasound and chest radiography for detecting pneumonia in children: a systematic review and meta-analysis. *Ital J Pediatr* 50:12
50. Llamas-Álvarez AM, Tenza-Lozano EM, Latour-Pérez J (2017) Accuracy of lung ultrasonography in the diagnosis of pneumonia in adults. *Chest* 151:374–382
51. Riccabona M (2008) Ultrasound of the chest in children (mediastinum excluded). *Eur Radiol* 18:390–399
52. Musolino AM, Tomà P, De Rose C et al (2022) Ten years of pediatric lung ultrasound: a narrative review. *Front Physiol* 12:721951
53. Kim OH, Kim WS, Kim MJ et al (2000) US in the diagnosis of pediatric chest diseases. *Radiographics* 20:653–671
54. Kang DWW, Campos JRMD, Andrade Filho LDO et al (2008) Thoracoscopy in the treatment of pleural empyema in pediatric patients. *J Bras Pneumol* 34:205–211
55. Islam S, Calkins CM, Goldin AB et al (2012) The diagnosis and management of empyema in children: a comprehensive review from the APSA Outcomes and Clinical Trials Committee. *J Pediatr Surg* 47:2101–2110
56. Bouhemad B, Brisson H, Le-Guen M et al (2011) Bedside ultrasound assessment of positive end-expiratory pressure-induced lung recruitment. *Am J Respir Crit Care Med* 183:341–347
57. Sameshima YT, de Almeida JFL, Silva MMA et al (2014) Ultrasound-guided lung recruitment in a 3-month-old infant with acute respiratory distress syndrome. *Ultrasound Q* 30:301–305

Publisher's Note Springer Nature remains neutral with regard to jurisdictional claims in published maps and institutional affiliations.

Springer Nature or its licensor (e.g. a society or other partner) holds exclusive rights to this article under a publishing agreement with the author(s) or other rightsholder(s); author self-archiving of the accepted manuscript version of this article is solely governed by the terms of such publishing agreement and applicable law.

Authors and Affiliations

Yoshino Tamaki Sameshima¹ · Andrés García-Bayce² · Fabiana Gual Oranges¹ · Marcelo Assis Rocha¹ · Márcia Wang Matsuoka¹ · Jovan Lovrenski^{3,4}

✉ Yoshino Tamaki Sameshima
kymjr@uol.com.br

Andrés García-Bayce
a.garcia.bayce@imagenologiapediatria.edu.uy

Fabiana Gual Oranges
fabianagual@gmail.com

Marcelo Assis Rocha
massisrocha@gmail.com

Márcia Wang Matsuoka
marciamatsuoka123@gmail.com

Jovan Lovrenski
jovan.lovrenski@mf.uns.ac.rs

¹ Diagnostic Imaging Department, Hospital Israelita Albert Einstein, Av. Albert Einstein, 627/701, 05652-900 São Paulo, SP, Brazil

² Imaging Department, Centro Hospitalario Pereira Rossell, Montevideo, Uruguay

³ Faculty of Medicine, University of Novi Sad, Novi Sad, Serbia

⁴ Radiology Department, Institute for Children and Adolescents Health Care of Vojvodina, Novi Sad, Serbia